Spatial correlation of an electron and a hole in a quasi-two-dimensional gas and its relationship to the scattering tensor

L. I. Korovin, I. G. Lang, and S. T. Pavlov

A. F. Ioffe Physicotechnical Institute, Russian Academy of Sciences, 194021 St. Petersburg, Russia

The spatial correlation of an electron and a hole generated by light in a quasi-two-dimensional electron gas is investigated in the linear approximation with respect to the intensity of the exciting light. The correlation is determined by the interaction of electrons and holes with LO phonons. The theory makes it possible to calculate the distribution function $F_N(\mathbf{r})$ (**r** is the two-dimensional vector of the relative motion of an electron and a hole, and N is the number of LO phonons emitted), as well as the function $F_N(\mathbf{r},\mathbf{K})$ (**K** is the wave vector of the motion of the center of mass of the respective electron–hole pair), which is related to the fourth-rank scattering tensor in multiphonon resonant Raman scattering. A calculation of $F_N(\mathbf{r})$ is performed for a quantum well of rectangular shape with infinitely high potential barriers in the approximation of a model interaction, which presumes the absence of a dependence of the interaction between the electron and an LO phonon on the wave vector of the phonon. Exact expressions are obtained for $F_N(\mathbf{r})$ within this approximation and in the heavy-hole approximation over a broad range of variation of the frequency of the exciting light, which includes both the resonant case, in which the electron drops to the minimum of the size-quantization band after the emission of an LO phonon, and the nonresonant case. © *1995 American Institute of Physics.*

1. INTRODUCTION

Multiphonon resonant Raman scattering is an effective tool for investigating quasi-two-dimensional electron structures, i.e., superlattices, quantum wells, and inversion layers.[1] The effect is confined to the appearance of a series of peaks in the scattered light, which are known as phonon replicas, at the frequencies $\omega_s = \omega_l - N\omega_{LO}$, where ω_s and ω_l are the frequencies of the scattered and exciting light, respectively, ω_{LO} is the frequency of the LO phonons, N is the number of the phonon replica, which is equal to the number of phonons emitted in the scattering process.[2] If the frequency ω_l is in the range of the fundamental absorption of the semiconductor, the intensity of the phonon replica is weakly dependent on N. This circumstance has made it possible to observe phonon replicas with large N: $N = 20$ for single-crystal InI (Ref. 3) and $N = 10$ for a system of quantum wells.[4]

There are two approaches to the theory of multiphonon resonant Raman scattering. In one of them the fourth-rank scattering tensor $S_{\alpha\beta\gamma\delta}$, which determines the scattering cross section, is calculated directly. A special diagram technique, which makes it possible to take into account the interaction of an electron with LO phonons in any order of perturbation theory, has been developed to calculate the scattering tensor, and the frequency dependence of the scattering cross section corresponding to the phonon replica with the number N has been calculated both in the absence of a magnetic field and in a strong magnetic field for a three-dimensional semiconductor system[5–7] and for a quasi-two-dimensional system.[8,9] The other approach is based on the calculation of the distribution function of electron–hole pairs with respect to the distance between the particles in each

pair. The spatial correlation of an electron and a hole is determined by their interaction with LO phonons and plays an important role in multiphonon resonant Raman scattering. This is illustrated by the following example. Let the absorption of a quantum of light with a frequency $\omega_l > \omega_g$ ($\hbar\omega_g = E_g$ is the width of the band gap) result in the appearance of an electron–hole pair and one LO phonon, which corresponds to the indirect creation of an electron–hole pair. Then the electron loses energy by generating LO phonons and directly annihilates with the same hole, if the scattering is treated in a linear approximation with respect to the intensity of the exciting light. When the intensity of the exciting light is increased, the electron can annihilate with "another" hole. Scattering which is nonlinear with respect to the exciting light will not be considered below. The reverse sequence of events is possible when an electron–hole pair is created directly without the emission of a phonon, and annihilation occurs indirectly with the virtual emission of the last phonon of a cascade. For simplicity, it is assumed that the hole is heavy and does not emit phonons. Since all the intermediate states of the scattering process, apart from the first or last state, are real, the generation of phonons results in real wandering of the electron with a mean free path $\lambda_e \propto \alpha^{-1}$, where α is the Fröhlich coupling constant. In a three-dimensional sample the most probable volume for wandering is approximately equal to $\lambda_e^3 \propto \alpha^{-3}$. In a quasi-two-dimensional system, in which the motion of an electron is confined to a plane, the wandering is restricted to a part of the plane having an area $\lambda_e^2 \propto \alpha^{-2}$, causing a sharp increase in the scattering efficiency in a two-dimensional system in comparison with a three-dimensional system. In fact, the scattering probability is proportional to the probability of the return of the electron to the point of creation of the electron–hole pair

after the emission of phonons, if it is assumed that the heavy hole remains at the site of creation of the pair. This probability is, in turn, inversely proportional to the dimensions of the region in which the electron wanders. Therefore, in a three-dimensional sample the scattering cross section corresponding to the Nth phonon replica is $\sigma_N \propto \alpha^3$, beginning at $N=4$ (Refs. 5 and 6), while in a quasi-two-dimensional system we have $\sigma_N \propto \alpha^2$ for $N \geq 3$, i.e., it increases by a factor of α^{-1} ($\alpha \ll 1$) in comparison with the three-dimensional case.[8]

It is seen from the example presented that the spatial correlation of an electron and a hole due to the generation of phonons during scattering plays a decisive role. If no such correlation exists, multiphonon resonant Raman scattering cannot occur. We stress that the we are dealing not with a Coulomb correlation, which produces exciton states, but with a correlation of a free electron and a free hole, which generate phonons.

For the sake of simplicity and clarity, the case of a very large hole effective mass is considered here. If the electron and hole effective masses m_e and m_h are comparable in value, the two particles created by light at a single point wander through the crystal, emitting LO phonons, and they can annihilate, if they encounter one another at a single point again. This is possible, since the mean free path of both particles is restricted. The result of the theory of multiphonon resonant Raman scattering for comparable values of m_e and m_h does not differ qualitatively from the case $m_h \gg m_e$. One exception is the case of very similar masses, in which the intensity of the multiphonon resonant Raman scattering increases sharply.[10–12]

The distribution function of electron–hole pairs in a three-dimensional semiconductor was obtained in Ref. 6 (in the absence of a magnetic field) and in Ref. 13 for a strong magnetic field. Since quasi-two-dimensional systems differ significantly from three-dimensional semiconductors and since these systems have aroused a great deal of interest, it would be useful to develop a systematic theory, which would make it possible to calculate the distribution function of electron–hole pairs for any number of phonons emitted.

A model of a quantum well, which is regarded as an example of a quasi-two-dimensional system, is formulated, the definition of the wave function of an electron–hole pair after the emission of N phonons is given, and the diagram-technique rules for calculating it are presented in Sec. 2. An expression for the wave function is derived in Sec. 3, and it is shown that it is an eigenfunction of the operator of the two-dimensional quasimomentum of the center of mass of the electron–hole pair. In Sec. 4 the distribution function of electron–hole pairs is introduced, and the diagram-technique rules for calculating it are presented. Section 5 is devoted to the derivation of general formulas for calculating the total number of pairs emitting N LO phonons. In Sec. 6 the relationship between the Fourier transform of the distribution function and the scattering tensor is established. Sections 7 and 8 are devoted to calculating the distribution function with $N=0$ for arbitrary electron and hole effective masses from $N \geq 1$ in the heavy-hole approximation.

2. MODEL OF A QUASI-TWO-DIMENSIONAL SYSTEM AND WAVE FUNCTION OF AN ELECTRON–HOLE PAIR

A theory is developed for a single rectangular quantum well with infinitely high walls in the case of satisfaction of the inequality $d \ll \lambda_e$, $\lambda_h [d$ is the width of the well and $\lambda_{e(h)}$ is the electron (hole) mean free path], which ensures quantization of the motion of the electron and the hole in the direction perpendicular to the plane of the well. If the well is demarcated by the $z=0$ and $z=d$ planes, in the effective-mass approximation the wave functions of the electron and the hole have the form

$$\psi_{\mathbf{k},n}(\mathbf{r},z) = S_0^{-1/s} \exp(i\mathbf{k} \cdot \mathbf{r}) \varphi_n(z), \tag{2.1}$$

where $\mathbf{r}$ is a two-dimensional vector in the plane of the well (the xy plane), $\mathbf{k}$ is a two-dimensional wave vector, S_0 is the normalization area, $n = 1, 2, \cdots$ denotes the electron (hole) size-quantization quantum numbers,

$$\varphi_n(z) = \sqrt{2/d} \sin(\pi n z/d) \quad \text{for} \quad 0 \leq z \leq d. \tag{2.2}$$

Outside of this range $\varphi_n(z) = 0$. The functions $\varphi_n(z)$ satisfy the orthogonality and normalization conditions

$$\int_{-\infty}^{\infty} \varphi_n(z) \varphi_{n'}(z) dz = \delta_{nn'}.$$

The energies of the electron and the hole are equal, respectively, to $\hbar \omega_e(\mathbf{k},n)$ and $E_g + \hbar \omega_h(\mathbf{k},n)$, where

$$\hbar \omega_{e(h)}(\mathbf{k},n) = \frac{\hbar^2}{2m_{e(h)}} \left(k^2 + \frac{\pi^2 n^2}{d^2} \right). \tag{2.3}$$

A system consisting of an electron–hole pair appearing as a result of the absorption of one photon with a frequency ω_l (in an allowed direct transition) and a certain number of LO phonons is considered. Low temperatures, at which optical phonons are not excited and the interaction of an electron and a hole with phonons results only in their emission, are assumed. The electron spin is not taken into account, since it is of no significance to the further discussion.

We consider the wave function $\Psi_N(\mathbf{r}_e, z_e, \mathbf{r}_h, z_h, Y)$ of a system in a state in which an electron–hole pair emits N phonons. We write it in the form

$$\Psi_N(\mathbf{r}_e, z_e, \mathbf{r}_h, z_h, Y) = \sum_{\{n_{\text{ph}}\}, g} \Psi_{n_{\text{ph}}}^g(\mathbf{r}_e, z_e, \mathbf{r}_h, z_h) \Psi_{n_{\text{ph}}}(Y), \tag{2.4}$$

where $\Psi_{n_{\text{ph}}}^g$ is the wave function of a system of N phonons corresponding to the state in which the occupation numbers of the phonons with the wave vectors $\mathbf{q}_1, \cdots, \mathbf{q}_N$ are equal to unity and the remaining occupation numbers are equal to zero. Here Y is the set of coordinates for the phonon subsystem. The subscript n_{ph} denotes the set of vectors $\mathbf{q}_1, \cdots, \mathbf{q}_N$, and

$$\sum_{\{n_{\text{ph}}\}} \cdots = (N!)^{-1} \sum_{\mathbf{q}_1, \cdots, \mathbf{q}_N} \cdots. \tag{2.5}$$

The function $\Psi_{n_{\text{ph}}}^g$ is calculated using the diagram technique. Its rules are as follows.

1. The photon line (dashed line) corresponds to the photon wave vector $\kappa_l = 0$. This line does not have correspond-
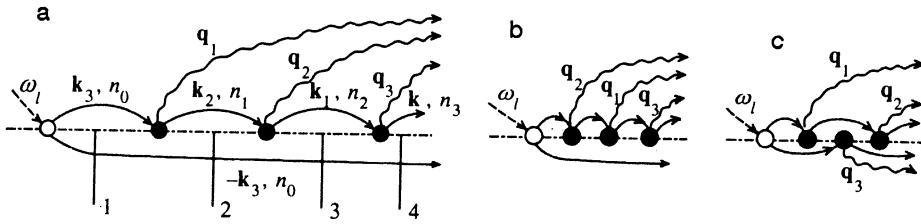
FIG. 1. Examples of diagrams corresponding to the wave function $\Psi^g_{n_{ph}}(r_e,z_e,r_h,z_h)$. $\mathbf{k}_1=\mathbf{k}+\mathbf{q}_{3\perp}$, $\mathbf{k}_2=\mathbf{k}+\mathbf{q}_{2\perp}+\mathbf{q}_{3\perp}$, $\mathbf{k}_3=\mathbf{k}+\mathbf{q}_{1\perp}+\mathbf{q}_{2\perp}+\mathbf{q}_{3\perp}$. The numbers 1–4 mark vertical sections.

ing vectors, but it determines the ratio between the wave vectors of the electron and hole lines adjacent to it.

2. The electron lines (solid lines) are shown above the line of the contour (dot-dashed line), and the hole lines (also solid) are shown below it. The electron and hole lines correspond to $\mathbf{k}$ and n, where $\mathbf{k}$ is a two-dimensional wave vector and n is the size-quantization number.

3. The phonon lines are wavy, and the three-dimensional wave vectors $\mathbf{q}$ correspond to them.

4. The law of the conservation of the transverse (in the plane of the well) components of the wave vectors holds at all the vertices (unfilled and filled points).

5. An unfilled point corresponds to the multiplier $M_l/\hbar$, where

$$M_l = -\sqrt{\frac{2\pi\hbar}{V_0}}\,\frac{e}{m_0}\mathbf{e}_l\cdot\mathbf{p}_{cv}\sqrt{\frac{u_l}{cn_l\omega_l}}, \tag{2.6}$$

V_0 is the normalization volume, e is the absolute value of the electron charge, m_0 is the free-electron mass, $\mathbf{e}_l$, u_l, and n_l are, respectively, the polarization vector of the exciting light, the group velocity, and the refractive index at the frequency ω_l, and $\mathbf{p}_{cv}$ is the interband matrix element of the electron momentum operator. The indices n of the electron and hole lines leaving an unfilled point coincide, and the vectors $\mathbf{k}$ are oppositely directed.

6. The filled points denote the vertices of the electron–phonon and hole–phonon interactions. A point at which an electron line $\mathbf{k},n$ enters and from which an electron line $\mathbf{k}-\mathbf{q}_\perp,n'$ and a phonon line $\mathbf{q}$ leaves corresponds to the multiplier

$$(-i/\hbar)C^*_q M_{nn'}(-q_z), \quad \mathbf{q}=(\mathbf{q}_\perp,q_z),$$

where

$$M_{nn'}(q_z)=\frac{2}{d}\int_0^d dz\,\exp(iq_z z)\sin\left(\frac{\pi n z}{d}\right)\sin\left(\frac{\pi n' z}{d}\right). \tag{2.7}$$

For the Fröhlich interaction

$$C_q = -i\hbar\omega_{LO}\sqrt{\frac{4\pi\alpha l^3}{V_0}}\,\frac{1}{ql}, \tag{2.8}$$

$$l=\sqrt{\frac{\hbar}{2m_e\omega_{LO}}}, \quad \alpha=\frac{e^2(\kappa_\infty^{-1}-\kappa_0^{-1})}{2\hbar\omega_{LO}l},$$

and κ_0 and κ_∞ are, respectively, the static and high-frequency dielectric constants of the crystal. In the case of the model interaction we have

$$C^Z_q = -i\sqrt{\frac{4\pi A l^3}{V_0}}\,\hbar\omega_{LO}\equiv C, \tag{2.9}$$

where A is a dimensionless coupling constant. A point at which a hole line $\mathbf{k},n$ enters and from which a hole line $\mathbf{k}-\mathbf{q}_\perp,n'$ and a phonon line $\mathbf{q}$ leave corresponds to the multiplier (2.8) or to (2.9) with the opposite sign, since the interaction of a hole with an LO phonon differs from the interaction of an electron only in sign and does not depend on the effective mass.

7. Each vertical section with the number j to the right of an unfilled point corresponds to the multiplier

$$\hbar/(E_i-E_j+i\hbar\gamma_j/2), \tag{2.10}$$

where $E_i=\hbar\omega_l$ is the initial energy, E_j is the sum of the energies, and γ_j is the sum of the reciprocal lifetimes corresponding to all the lines passing through a given cross section from left to right. The reciprocal lifetime of an electron in the state $\mathbf{k},n$ is denoted by $\gamma_e(\mathbf{k},n)$, and that of a hole is denoted by $\gamma_h(\mathbf{k},n)$.

8. Electron and hole lines with a free end and the indices $\mathbf{k},n$ correspond to the wave functions (2.1).

9. The summation is carried out over all the vectors $\mathbf{k}$ and indices n.

Examples of diagrams for three-phonon scattering ($N=3$) with different g are presented in Fig. 1. The index g indicates the type of diagram. We stress that a diagram of type g is characterized by fixed values of the wave vectors $\mathbf{q}_1,\cdots,\mathbf{q}_N$, so that, for example, diagrams 1a and 1b, which are distinguished by transposition of the vectors $\mathbf{q}_1$ and $\mathbf{q}_2$ are different. In Fig. 1c a phonon with a wave vector $\mathbf{q}_3$ is emitted by the hole. It can be emitted before a phonon with $\mathbf{q}_1$ or after a phonon with $\mathbf{q}_2$. These alternatives also correspond to different g, and they should be taken into account.

3. GENERAL EXPRESSION FOR THE WAVE FUNCTION OF AN ELECTRON–HOLE PAIR

Instead of the coordinates r_e,z_e,r_h,z_h of the electron and the hole, we introduce the coordinates of the center of mass and the relative motion:

$$\mathbf{R}=\frac{m_e\mathbf{r}_e+m_h\mathbf{r}_h}{M}, \quad Z=\frac{m_e z_e+m_h z_h}{M}, \quad \mathbf{r}=\mathbf{r}_e-\mathbf{r}_h,$$

$$z=z_e-z_h, \quad M=m_e+m_h.$$

We write the wave function corresponding to a diagram of type g in the following form:

$$\Psi_{n_{ph}}^g = \sum_{k_e,k_h} \sum_{n,m} C_{k_e,k_h,n,m,n_{ph}}^g \Psi_{k_e,k_h,n,m}(\mathbf{R},Z,\mathbf{r},z), \quad (3.1)$$

where $\mathbf{k}_e$, n and $\mathbf{k}_h$, m are the indices of the free electron and hole lines. Clearly, the wave function (3.1) is the result of superposition of the wave functions of free (not interacting with phonons) electron–hole pairs. For $\hbar\omega_l < E_g$, which corresponds to nonresonant scattering, $\gamma_{e(h)}$ in expression (2.10) can be disregarded, since we always have $\mathrm{Re}(E_i - E_j + i\hbar\gamma_j/2) \neq 0$. In this case ordinary perturbation theory with respect to the electron–phonon coupling constant is employed. However, when a crystal is illuminated in the region of its fundamental absorption, where the intermediate states are real, rather than virtual, ordinary perturbation theory is not applicable, and restructuring of the perturbation theory series is necessary in order that the quantities $\gamma_{e(h)}$, which are proportional to the electron–phonon coupling constant, would appear in the cross sections. Just such a restructured perturbation theory is used in the present work.

The coefficients $C_{k_e,k_h,n,m,n_{ph}}^g$ contain the Kronecker delta $\delta_{\mathbf{K},-\mathbf{Q}}$, where

$$\mathbf{K} = \mathbf{k}_e + \mathbf{k}_h, \quad \mathbf{Q} = \sum_{i=1}^N \mathbf{q}_{i\perp},$$

which follows from conservation of the transverse components of the wave vectors. In fact, if the initial transverse quasimomentum of the system is equal to zero (since $\kappa_i = 0$), in each vertical section, i.e., in an intermediate state of the system, the total transverse quasimomentum is also equal to zero, as can easily be verified on the diagrams. This also applies to the extreme right-hand section, in which the total wave vector of the electron–hole pairs equals $\mathbf{K}$ and the total transverse wave vector of the phonons equals $\mathbf{Q}$. Thus, the condition

$$\mathbf{K} + \mathbf{Q} = 0 \quad (3.2)$$

is satisfied. For the wave function $\Psi_{k_e,k_h,n,m}$ appearing on the right-hand side of (3.1) we easily obtain the expression

$$\Psi_{k_e,k_h,n,m} = S_0^{-1}\exp[i(\mathbf{K}\cdot\mathbf{R} + \mathbf{k}\cdot\mathbf{r})]$$

$$\times \varphi_n\left(Z + \frac{m_h}{M}z\right)\varphi_m\left(Z - \frac{m_e}{M}z\right), \quad (3.3)$$

$$\mathbf{k} = (m_h\mathbf{k}_e - m_e\mathbf{k}_h)/M$$

is the wave vector of the relative motion of the electron and hole.

On the right-hand side of (3.1) we pass from summation with respect to $\mathbf{k}_e$ and $\mathbf{k}_h$ to summation with respect to $\mathbf{K}$ and $\mathbf{k}$, using the relations

$$\mathbf{k}_e = \mathbf{k} + (m_e/M)\mathbf{K}, \quad \mathbf{k}_h = -\mathbf{k} + (m_h/M)\mathbf{K}. \quad (3.4)$$

Summing with respect to $\mathbf{K}$, with consideration of (3.2) we obtain

$$\Psi_{n_{ph}}^g = S_0^{-1}e^{-i\mathbf{Q}\cdot\mathbf{R}}\sum_{k,n,m} e^{i\mathbf{k}\cdot\mathbf{r}}C_{k-(m_e/M)\mathbf{Q},-k-(m_h/M)\mathbf{Q},n,m,n_{ph}}^g$$

$$\times \varphi_n\left(Z + \frac{m_h}{M}z\right)\varphi_m\left(Z - \frac{m_e}{M}z\right). \quad (3.5)$$

Function (3.5) is an eigenfunction of the momentum operator $(\hbar/i)\partial/\partial\mathbf{R}$ of the center of mass of the electron–hole pair in the plane of the quantum well. It corresponds to the eigenvalue $\mathbf{K} = -\mathbf{Q}$.

4. DISTRIBUTION FUNCTION OF ELECTRON–HOLE PAIRS WITH RESPECT TO THE RELATIVE-MOTION COORDINATE

We introduce the distribution function of pairs with respect to the relative-motion coordinate F_N after the emission of N LO phonons. This function is defined as

$$F_N(\mathbf{r},z) = \int d\mathbf{R}\int dZ\int dY|\Psi_N(\mathbf{r}_e,z_e,\mathbf{r}_h,z_h,Y)|^2 \quad (4.1)$$

and is the diagonal part of the density matrix of electron–hole pairs which have emitted N phonons. Using (2.4), we first of all integrate with respect to Y. Taking into account the orthonormality of the wave functions, we represent F_N in the form

$$F_N(\mathbf{r},z) = \sum_{\{n_{ph}\}}\sum_{g,g'}\int (\Psi_{n_{ph}}^{g'})^*\Psi_{n_{ph}}^g d\mathbf{R}\,dZ. \quad (4.2)$$

Substituting the wave functions (3.5) into (4.2) and integrating with respect to $\mathbf{R}$ and Z, we obtain

$$F_N(\mathbf{r},z) = \sum_{n,m,n'm'} F_{Nnmn'm'}(\mathbf{r})\xi_{nmn'm'}(z), \quad (4.3)$$

where

$$F_{Nnmn'm'}(\mathbf{r}) = \sum_{\mathbf{K}} F_{Nnmn'm'}(\mathbf{r},\mathbf{K}), \quad (4.4)$$

$$F_{Nnmn'm'}(\mathbf{r},\mathbf{K}) = S_0^{-1}\sum_{\mathbf{K},\mathbf{k}'} \exp[i(\mathbf{k}-\mathbf{k}')\mathbf{r}]\sum_{\{n_{ph}\}}\sum_{g,g'}$$

$$\times C_{k+(m_e/M)\mathbf{K},-k+(m_h/M)\mathbf{K},n,m,n_{ph}}^g$$

$$\times C_{k'+(m_e/M)\mathbf{K},-k'+(m_h/M)\mathbf{K},n',m',n_{ph}}^{g'*}, \quad (4.5)$$

$$\xi_{nmn'm'}(z) = \int_{-\infty}^{\infty} dZ\varphi_n\left(Z + \frac{m_h}{M}z\right)\varphi_m\left(Z - \frac{m_e}{M}z\right)$$

$$\times \varphi_{n'}\left(Z + \frac{m_h}{M}z\right)\varphi_{m'}\left(Z - \frac{m_e}{M}z\right).$$

The physical meaning of F_N is as follows: $F_N d\mathbf{r}\,dz$ is the number of pairs which have emitted N LO phonons in the ranges from $\mathbf{r}$ to $\mathbf{r} + d\mathbf{r}$ and from z to $z + dz$ normalized to one photon of exciting light. Integrating (4.3) with respect to z, it is easy to see that
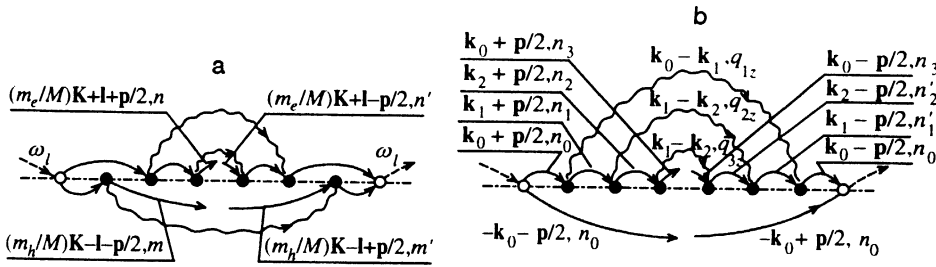
FIG. 2. Two diagrams corresponding to the distribution function $\mathscr{F}_{3nmn'm'}(\mathbf{p},\mathbf{K})$: a—the vectors $\mathbf{K}$ and $\mathbf{p}$, as well as the size-quantization numbers, are fixed; b—the case of $\mathbf{K}=0$, which is important for calculating the scattering tensor.

$$\int_{-\infty}^{\infty} \xi_{nmn'm'}(z)dz = \delta_{nn'}\delta_{mm'}. \qquad (4.6)$$

Therefore, the distribution function of the pairs with respect to the coordinate $\mathbf{r}$ equals

$$F_N(\mathbf{r}) = \int F_N(\mathbf{r},z)dz = \sum_{n,m} F_{Nnmnm}(\mathbf{r}) = \sum_{\mathbf{K}} F_N(\mathbf{r},\mathbf{k}); \qquad (4.7)$$

$$F_N(\mathbf{r},\mathbf{K}) = \sum_{n,m} F_{Nnmnm}(\mathbf{r},\mathbf{K}). \qquad (4.8)$$

Using (4.5), we determine the Fourier transform of $F_{Nnmn'm'}(\mathbf{r},\mathbf{K})$. In (4.5) we introduce the new variables $\mathbf{p}=\mathbf{k}-\mathbf{k}'$ and $\mathbf{l}=(\mathbf{k}+\mathbf{k}')/2$. Then

$$F_{Nnmn'm'}(\mathbf{r},\mathbf{K}) = S_0^{-1}\sum_{\mathbf{p}} \exp[i\mathbf{p}\cdot\mathbf{r}]\mathscr{F}_{Nnmn'm'}(\mathbf{p},\mathbf{K}), \qquad (4.9)$$

where

$$\mathscr{F}_{Nnmn'm'}(\mathbf{p},\mathbf{K}) = \sum_{\mathbf{l}} \sum_{g,g'} \sum_{\{n_{ph}\}} C_\eta^g (C_{\eta'}^{g'})^*, \qquad (4.10)$$

$$\eta = \mathbf{l}+(\mathbf{p}/2)+(m_e/M)\mathbf{K}, -\mathbf{l}-\mathbf{p}/2$$
$$+ (m_h/M)\mathbf{K}, n, m, n_{ph},$$

$$\eta' = \mathbf{l}-(\mathbf{p}/2)+(m_e/M)\mathbf{K}, -\mathbf{l}+\mathbf{p}/2$$
$$+ (m_h/M)\mathbf{K}, n', m', n_{ph}.$$

This Fourier transform can be visualized using diagrams, examples of which are presented in Fig. 2. The rules for the left-hand sides of the diagrams are the same as in Sec. 2, except for rule 8, i.e., the wave function does not correspond to the free ends of the electron and hole lines. The contribution of the right-hand sides of the diagrams is distinguished from the contribution of the left-hand side by complex conjugation. The vectors $\mathbf{K}$ and $\mathbf{p}$, as well as the indices n,m,n',m' are fixed, and the summation is carried out with respect to the vector $\mathbf{l}$, all the vectors $\mathbf{q}_i$, the internal indices, and the types of diagrams. The contributions of the diagrams which are distinguished only by transposition of the $\mathbf{q}_i$ compensate the multiplier $(N!)^{-1}$. Therefore, this multiplier need not be written, and the transposition of the phonon vectors need not be taken into account in the diagram [see Eq. (2.5)].

Calculating $\mathscr{F}_{Nnmn'm'}$ by the diagram technique and using (4.7) and (4.9), we obtain the distribution $F_N(\mathbf{r})$. When the function $F_{Nnmn'm'}(\mathbf{r})$ defined in (4.4) and (4.9) is calcu-

lated, it should be recalled that $\Psi_{n_{ph}}^g$ contains the Kronecker delta $\delta_{\mathbf{K},-\mathbf{Q}}$, which eliminates the summation with respect to $\mathbf{K}$ in (4.4). For example, if $N=0$, then $\mathbf{K}=-\mathbf{Q}=0$ and $F_{0nmnm}(\mathbf{r})$ is represented by a double sum with respect to the vectors $\mathbf{p}$ and $\mathbf{l}$. In the case of $N=1$, the set $\mathbf{q}_1, \cdots, \mathbf{q}_N$ reduces $\mathbf{q}_1$, and $\mathbf{q}_{1\perp}=\mathbf{Q}=-\mathbf{K}$. Then $F_{1nmnm}(\mathbf{r})$ is a triple sum with respect to $\mathbf{p}$, $\mathbf{l}$, and $\mathbf{q}_{1\perp}$. An increase in the number of phonons emitted by unity adds summation with respect to $\mathbf{q}$.

5. TOTAL NUMBER OF ELECTRON–HOLE PAIRS WHICH HAVE EMITTED N LO PHONONS

According to the definition (4.1), the total number of electron–hold pairs which have emitted N LO phonons

$$\mathscr{N}_N = \int d\mathbf{r} \int dz F_N(\mathbf{r},z).$$

Using (4.3) and (4.6), we obtain

$$\mathscr{N}_N = \sum_{n,m} \int d\mathbf{r} \int dz F_{Nnmnm}(\mathbf{r}). \qquad (5.1)$$

Taking into account (4.4) and (4.5), we represent $\mathscr{N}_N$ in the following form:

$$\mathscr{N}_N = \sum_{\mathbf{K}} \mathscr{N}_N(\mathbf{K}), \quad \mathscr{N}_N(\mathbf{K}) = \sum_{\{n_{ph}\}} \sum_{n,m} \sum_{\mathbf{k}} \left|\sum_g C_\eta^g\right|^2,$$

where the vector $\mathbf{l}+\mathbf{p}/2$ in the index η defined in (4.10) has been replaced by $\mathbf{k}$. The function $\mathscr{N}_N(\mathbf{K})$ gives the number of pairs which have emitted N LO phonons and for which the wave vector of the motion of the center of mass equals $\mathbf{K}$. The number of pairs is expressed in terms of the Fourier transform of the distribution function (4.10):

$$\mathscr{N}_N(\mathbf{K}) = \sum_{n,m} \mathscr{F}_{Nnmnm}(\mathbf{p}=0,\mathbf{K}). \qquad (5.2)$$

The total number of pairs (5.1) is expressed in terms of the function

$$\mathscr{F}_{Nnmnm}(\mathbf{p}) = \sum_{\mathbf{K}} \mathscr{F}_{Nnmnm}(\mathbf{p},\mathbf{K}) \qquad (5.3)$$

using the formula

$$\mathscr{N}_N = \sum_{n,m} \mathscr{F}_{Nnmnm}(\mathbf{p}=0), \qquad (5.4)$$

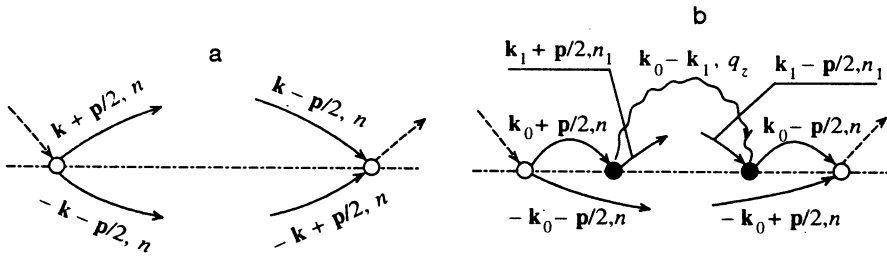where $\mathscr{F}_{Nnmnm}(\mathbf{p}=0)=\mathscr{N}_{Nnm}$ corresponds to the number of such pairs emitting N phonons in which the electron is found in the size-quantization band with the index n and the hole is in band m.

6. RELATIONSHIP OF THE DISTRIBUTION FUNCTION TO THE SCATTERING TENSOR

The probability of the emission of a quantum of secondary radiation per unit time normalized to one photon of exciting light is defined by the expression

$$\bar{W}_{sN}=\frac{2\pi}{\hbar}\sum_f |\langle f|M_s|i\rangle|^2 \delta(\hbar\omega_l-\hbar\omega_s-N\hbar\omega_{LO}). \quad (6.1)$$

In the effective-mass approximation the interaction of light with the electron system is specified by the constant (2.6), in which the index l for the exciting light must be replaced by the index s for the scattered light. The initial state of the system is described by the function (2.4), and the final state is described by the function

$$\Psi_f=\delta(\mathbf{r}_e-\mathbf{r}_h)\delta(z_e-z_h)\Psi_{n_{ph}}(Y), \quad (6.2)$$

which is characterized by the presence of N phonons with the set of wave vectors n_{ph}. The summation over the states in (6.1) signifies summation over the sets n_{ph}.

Using (2.4), (3.1), and (6.2) and taking into account the relation

$$\int_{-\infty}^{\infty}dZ\int_{-\infty}^{\infty}dz\; \varphi_n\!\left(Z+\frac{m_h}{M}z\right)\varphi_m\!\left(Z-\frac{m_e}{M}z\right)\delta(z)=\delta_{n,m},$$

we obtain

$$\langle f|M_s|i\rangle=M_s\sum_{\mathbf{k},n}\sum_g C^g_{\mathbf{k},-\mathbf{k},n,n,n_{ph}}. \quad (6.3)$$

Plugging (6.3) into (6.1) gives

$$\bar{W}_{sN}=\frac{2\pi}{\hbar}|M_s|^2\delta(\hbar\omega_l-\hbar\omega_s-N\hbar\omega_{LO})$$

$$\times\sum_{\mathbf{k},\mathbf{k}',n,n'}\sum_{\{n_{ph}\}}\sum_{g,g'} C^g_{\mathbf{k},-\mathbf{k},n,n,n_{ph}}C^{g'*}_{\mathbf{k}',-\mathbf{k}',n',n',n_{ph}}. \quad (6.4)$$

Comparing (6.2) and (4.5), we obtain the relation

$$\bar{W}_{sN}=\frac{2\pi}{\hbar}|M_s|^2\delta(\hbar\omega_l-\hbar\omega_s-N\hbar\omega_{LO})$$

$$\times S_0\sum_{n,n'} F_{Nnn'n'}(\mathbf{r}=0,\mathbf{K}=0). \quad (6.5)$$

Thus, the relationship between the probability of secondary emission and the functions $F_{Nnnn'n'}(\mathbf{r},\mathbf{K})$ appearing in (4.3) has been obtained. Now we can relate $\bar{W}_{sN}$ to the scattering tensor $S_{\alpha\beta\gamma\delta}$, which was derived for the three-dimensional case in Refs. 14–16 and for a quasi-two-dimensional system in Ref. 8. According to Ref. 16,

$$\bar{W}_{sN}=\frac{(2\pi)^3}{V_0}\frac{u_lu_s}{c^2n_ln_s}\; \omega_l\omega_s e^*_{s\alpha}e_{l\gamma}e_{s\beta}e^*_{l\lambda}S_{\alpha\gamma\beta\lambda}, \quad (6.6)$$

where $\mathbf{e}_s$ and $\mathbf{e}_l$ are the polarization vectors of the scattered and exciting light, u_l and u_s are the group velocities of light, and n_l and n_s are the refractive indices at the frequencies ω_l and ω_s, respectively.

Equations (6.5) and (6.6) can be used to establish the correspondence between the convolution of the scattering tensor with the polarization vectors, on the one hand, and the functions $F_{Nnnn'n'}(\mathbf{r}=0,\mathbf{K}=0)$, on the other hand, which are related to $F_N(\mathbf{r},z)$ by Eqs. (4.3)–(4.5). If we pass from $F_N(\mathbf{r},z)$ to $F_N(\mathbf{r})$ by means of Eq. (4.7), we find that the scattering tensor is related to $F_{Nnnn'n'}(\mathbf{r},\mathbf{K})$, while $F_N(\mathbf{r})$ is determined by $F_{Nnn'nn'}(\mathbf{r},\mathbf{K})$. This finding differs from the result obtained in Ref. 6 for the three-dimensional case, in which the scattering tensor is related directly to the function $F_N(\mathbf{r}=0,\mathbf{K}=0)$, where $\mathbf{r}$ and $\mathbf{K}$ are three-dimensional vectors. In the quasi-two-dimensional system such a relationship is realized only for contributions to the distribution function and the scattering tensor which are diagonal with respect to the indices n, i.e., when the four indices coincide.

7. DISTRIBUTION FUNCTION OF ELECTRON–HOLE PAIRS BEFORE THE EMISSION OF PHONONS

As an example we calculate the distribution of electron–hole pairs for the $N=0$ case. Then Eqs. (4.7), (4.8), and (4.9) lead to the relations

$$F_0(\mathbf{r})=\sum_n F_{0n}(\mathbf{r}), \quad F_{0n}(\mathbf{r})=S_0^{-1}\sum_{\mathbf{p}}$$

$$\times\exp(i\mathbf{p}\cdot\mathbf{r})\mathscr{F}_{0n}(\mathbf{p}), \quad F_{0n}\equiv F_{0nnnn}, \quad (7.1)$$

where $\mathscr{F}_{0n}(\mathbf{p})$ is understood to be $\mathscr{F}_{0nnnn}(\mathbf{p},\mathbf{K}=0)$. The corresponding diagram is presented in Fig. 3a. The real function $\mathscr{F}_{0n}(\mathbf{p})$ is represented in the form

$$\mathscr{F}_{0n}(\mathbf{p})=|M_l|^2\left(\frac{2\mu}{\hbar^2}\right)^2\sum_{\mathbf{k}}\left[\left(\mathbf{k}+\frac{\mathbf{p}}{2}\right)^2-K_0^2-iQ_0^2\right]^{-1}$$

$$\times\left[\left(\mathbf{k}-\frac{\mathbf{p}}{2}\right)^2-K_0^2+iQ_0^2\right]^{-1}, \quad (7.2)$$

$$K_0^2 \equiv K_0^2(n) = \frac{1}{\hbar^2}\left[2\mu(\hbar\omega_l - E_g) - \frac{\hbar^2\pi^2 n^2}{d^2}\right]. \qquad (7.3)$$

If $K_0^2 \geqslant 0$ holds, $K_0(n)$ has the meaning of the magnitude of the wave vector of the relative motion of an electron and a hole which are found in the $n_e = n_h = n$ size-quantization bands after creation of an electron–hole pair. The wave vectors of the electron and the hole are equal to $\mathbf{k}_0$ and $-\mathbf{k}_0$, respectively, whence it follows, according to Eq. (3.3) that $\mathbf{k}_0 = \mathbf{k}$. The quantity

$$Q_0^2 \equiv Q_0^2(n) = (\mu/\hbar)[\gamma_e(K_0,n) + \gamma_h(K_0,n)] \qquad (7.4)$$

characterizes the nonstationary nature of the state of an electron–hole pair due to the generation of LO phonons. If $K_0 \neq 0$, Q_0^2 can be represented in the form of a ratio:

$$Q_0^2 = K_0/\lambda_0, \quad \lambda_0 = v\tau_0,$$

$$\tau_0 = \gamma_0^{-1} = [\gamma_e(K_0,n) + \gamma_h(K_0,n)]^{-1}, \quad v = \hbar K_0/\mu, \qquad (7.5)$$

where λ_0 is the mean free path in terms of the relative motion, τ_0 is the lifetime of the pair in the particular state until the emission of an LO phonon, and v is the rate of the

relative motion. Strictly speaking, γ_e, γ_h, and Q_0^2 depend on the wave vector $\mathbf{k}$. Since the value of Q_0^2 is small, it is reasonable to take it into account only in the region of $\mathbf{k}$ where $k^2 = K_0^2$. Therefore, with good accuracy, Q_0^2 is a constant which depends on K_0. After such an approximation the sum in (7.2) is calculated exactly. Passing from summation to integration and performing the replacement of variables $\mathbf{k} + \mathbf{p}/2 = \boldsymbol{\eta}$, we represent $\mathscr{F}_{0n}(\mathbf{p})$ in the form

$$\mathscr{F}_{0n}(\mathbf{p}) = \frac{S_0 |M_l|^2}{2\pi}\left(\frac{2\mu}{\hbar^2}\right)^2 \Phi_n(p), \qquad (7.6)$$

where $\Phi_n(p)$ is represented by a double integral, which is calculated exactly:

$$\Phi_n(p) = \int_0^\infty \eta \, d\eta \, [\eta^2 - K_0^2 - iQ_0^2]^{-1} \int_0^{2\pi} d\varphi[\eta^2 + p^2$$

$$- 2p\eta \, \cos\varphi - K_0^2 + iQ_0^2]^{-1}. \qquad (7.7)$$

Integrating first with respect to the angle φ and then with respect to the variable η, we obtain the expression for $\Phi_n(p)$:

$$\Phi_n(p) = g_n/\sqrt{p^2 + y_-^{(n)}}, \quad g_n = g_n'/\sqrt{|p^2 - y_+^{(n)}|},$$

$$g_n' = \begin{cases} \arctan\left[\sqrt{(p^2 + y_-^{(n)})(y_+^{(n)} - p^2)}/(p^2 - 2K_0^2)\right], & p^2 \leqslant y_+^{(n)}, \\ \ln\left[(p^2 - 2K_0^2 + \sqrt{(p^2 + y_-^{(n)})(p^2 - y_+^{(n)})})/(2\sqrt{K_0^4 + Q_0^4})\right], & p^2 \geqslant y_+^{(n)}, \end{cases}$$

$$y_\pm^{(n)} = 2(\sqrt{K_0^4 + Q_0^4} \pm K_0^2). \qquad (7.8)$$

In (7.8) we have $0 \leqslant \arctan x \leqslant \pi$, i.e., $\arctan(+0)=0$, $\arctan(-0) = \pi$, $\arctan(\pm\infty) = \pi/2$. Using the definition of F_{0n} (7.1), we obtain

$$F_0(\mathbf{r}) = S_0|M_l|^2(2\pi)^{-3}\left(\frac{2\mu}{\hbar^2}\right)^2$$

$$\times \int_0^\infty p \, dp \, \Phi_n(p) \int_0^{2\pi} d\varphi \, \exp(ipr\cos\varphi). \qquad (7.9)$$

Integration with respect to φ in (7.9) gives $2\pi J_0(pr)$, where J_0 is a Bessel function. Plugging in $\Phi_n(p)$ from (7.8), we represent F_{0n} in the form of a single integral:

$$F_{0n}(\mathbf{r}) = S_0|M_l|^2(2\pi)^{-2}(2\mu/\hbar^2)^2 V_{0n}(r),$$

$$V_{0n}(r) = \int_0^\infty p \, dp(p^2 + y_-^{(n)})^{-1/2}g_n J_0(pr). \qquad (7.10)$$

Integrating over the entire plane of the quantum well, we obtain the total number of electron–hole pairs which have not emitted even one phonon:

$$\mathscr{N}_0 = \sum_n \mathscr{N}_{0n}, \quad \mathscr{N}_{0n} = \int F_{0n}(\mathbf{r})d\mathbf{r} = \mathscr{F}_{0n}(\mathbf{p}=0).$$

It follows from (7.6) that

$$\mathscr{N}_{0n} = W_l[\gamma_e(K_0,n) + \gamma_h(K_0,n)]^{-1}\pi^{-1}$$

$$\times \arctan(-Q_0^2/K_0^2), \qquad (7.11)$$

where $W_l = \hbar^{-3}S_0|M_l|^2\mu$ is the probability of the direct creation of a pair per unit time under the condition $K_0^2 \gg Q_0^2$. If $K_0^2 \ll Q_0^2$ holds, $\mathscr{N}_{0n}$ decreases by a factor of 2.

The distribution function $f_{0n}(\mathbf{r})$ normalized to unity equals

$$f_{0n}(\mathbf{r}) = \mathscr{N}_{0n}^{-1}F_{0n}(\mathbf{r}) = \frac{Q_0^2}{\pi}\left[\arctan\left(\frac{-Q_0^2}{K_0^2}\right)\right]^{-1} V_{0n}(r). \qquad (7.12)$$

The function V_{0n} diverges in the limiting case $r \to 0$ as $[\ln(rK_0)]^2$, if the inequality $(K_0/Q_0) \gg 1$ holds (the nonresonant case). In the resonant case $[(K_0/Q_0) \leqslant 1]$ the function V_{0n} diverges as $[\ln(rQ_0)]^2$. In this case, as is seen from (2.3), $\omega_l = \omega_g + \hbar\pi^2 n^2/2\mu d^2$, i.e., after the absorption of a quantum of light, the electron and the hole are at the extrema of the size-quantization bands. Let us consider these cases in greater detail

If $K_0 \gg Q_0$ holds, then we have $y_+^{(n)} \approx 4K_0^2$, $y_-^{(n)} \approx \lambda_0^{-2} = Q_0^4/K_0^2$, and the function g_n decreases slowly from $g_n(0) = \pi/2K_0$ to $g_n(4K_0^2) = K_0^{-1}$. In the limit $p \to \infty$ we obtain $g_n \to p^{-1}\ln(p/K_0)$. The replacement of $g_n(p^2)$ by
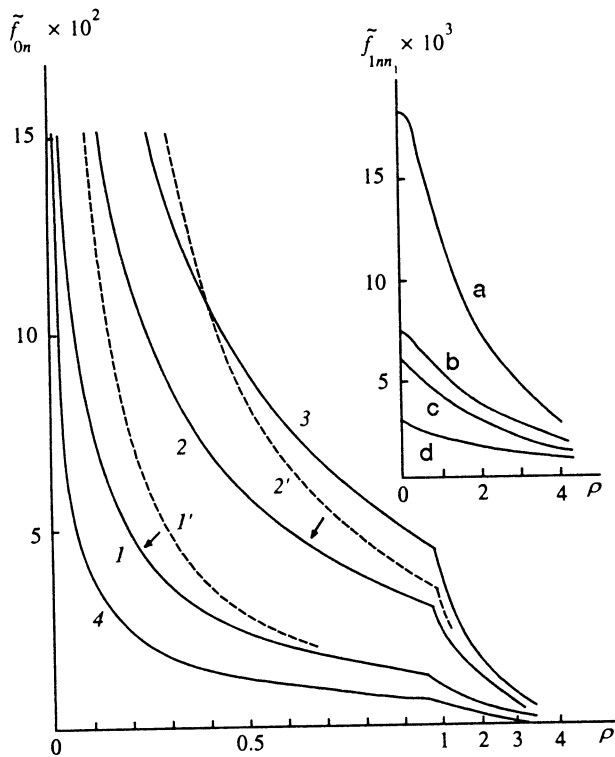
FIG. 4. Coordinate dependence of the distribution function $f_{0n}(\mathbf{r})$ before phonon emission $(\rho=r/l_0$, $\tilde{f}_{0n}=f_{0n}l_0^2$, $\tilde{f}_{1nn_1}=f_{1nn_1}l_0^2$, $\Omega_j=K_j^2l_0^2$, $\Gamma_j=Q_j^2l_0^2$, $j=0$, 1). Curves 1-3 were obtained for $\Gamma_0=0.1$ and $\Omega_0=1$ (1), 0.1 (2), and 0 (3). Curves $1'$ and $2'$ were calculated from the approximate equation (7.13). The arrows point out correspondence to exact curves. Curve 4 was obtained for $\Gamma_0=0.1$ and $\Omega_0=1$, and its vertical scale was increased five fold. Inset: coordinate dependence of the distribution function $f_{1nn_1}(\mathbf{r})$ after the emission of one phonon for $\Gamma_0=\Gamma_1=0.1$ when $\Omega_0=\Omega_1=0$ (curve a), $\Omega_0=0$, $\Omega_1=0.5$ (curve b), $\Omega_0=1$, $\Omega_1=0$ (curve c), and $\Omega_0=1$, $\Omega_1=0.5$ (curve d); $\mu\to m_e$.

$g_n(0)$, which corresponds to the polar approximation employed in Ref. 6, gives the following expression for $f_{0n}(\mathbf{r})$:

$$f_{0n}(\mathbf{r})=(2\pi\lambda_0 r)^{-1}\exp(-r/\lambda_0). \qquad (7.13)$$

We note that the replacement of $g_n(p^2)$ by a constant alters the behavior of the integrand at large p. This accounts for the stronger divergence of $f_{0n}(\mathbf{r}\to0)$ than that observed in the exact expression (7.12) with the function (7.10). The function (7.13) is valid when $K_0 r\gg1$. At resonance we have $K_0=0$ and $y_{\pm}^{(n)}=2Q_0^2$. The behavior of $f_{0n}(\mathbf{r})$ is determined by a single characteristic length $\Lambda_0=(\sqrt{2}Q_0)^{-1}$ $=\sqrt{\hbar/2\mu\gamma_0}$. If $r\ll\Lambda_0$ holds, we have $f_{0n}(\mathbf{r})\propto[\ln(r/\Lambda_0)]^2$. The decrease in the function (7.13) for the nonresonant case is specified by $\lambda_0=\hbar K_0\tau_0/\mu$. The ratio $\lambda_0/\Lambda_0=K_0/Q_0$ is much greater than unity, i.e., the resonant distribution function decreases more rapidly than the nonresonant analog. The length λ_0 is a classical parameter, while Λ_0 is a quantum parameter, since $Q_0^{-2}\propto\hbar$. Figure 4 presents the coordinate dependence $f_{0n}(\mathbf{r})$ for several values of the dimensionless parameters $\Omega_0=K_0^2l_0^2$ and $\Gamma_0=Q_0^2l_0^2=\gamma_0/2\omega_{\mathrm{LO}}$, where $l_0^2=\hbar/2\mu\omega_{\mathrm{LO}}$.

The condition $K_0^2\geq0$ corresponds to a frequency in the fundamental absorption region. However, Eq. (7.12) also has meaning for $K_0^2<0$, where the creation of an electron–hole pair is virtual. In the near-resonant region ($|K_0|^2\lesssim Q_0^2$) the results differ only slightly from those corresponding to the case of $K_0^2>0$, since a pair can actually be created by means of transitions between the "tails" of the density of states in the two-dimensional bands. But $|K_0|^2\gg Q_0^2$ holds and the contribution of the real processes can be neglected, then, setting $Q_0=0$ in (7.12), we obtain

$$f_{0n}(\mathbf{r})=2|K_0|^2\pi^{-1}\int_0^\infty\frac{dx}{\sqrt{1+x^2}}J_0(2|K_0|rx)\ln(x+\sqrt{1+x^2}).$$
$$(7.14)$$

It is seen from (7.14) that $f_{0n}(\mathbf{r})$ diverges at small $\mathbf{r}$ as $[\ln(|K_0|r)]^2$, and its decrease with increasing $\mathbf{r}$ is determined by $2|K_0|^{-1}$. An equation similar to (7.13) is obtained under the approximation $2x^{-1}\ln(x+\sqrt{1+x^2})\to1$:

$$f_{0n}(\mathbf{r})=(|K_0|/\pi r)\exp(-2|K_0|r). \qquad (7.15)$$

The ratio between the exponents in (7.15) and (7.13) is equal to $2\lambda_0|K_0|\gg1$, i.e., the distribution function decreases very rapidly with increasing $\mathbf{r}$. In other words, the size of the pair in a virtual transition is of the same order as the wavelength of the relative motion of the electron and the hole and is small compared with that in a real transition. The quantity $|K_0|$ is related to the energy deficiency in a virtual transition:

$$\Delta E=E_g+\frac{\hbar^2\pi^2n^2}{2\mu d^2}-\hbar\omega_l=\frac{\hbar|K_0|^2}{2\mu}.$$

Hence the lifetime of a pair in a virtual state can be estimated:

$$\Delta t\simeq\frac{\hbar}{\Delta E}=\frac{2\mu}{\hbar|K_0|^2},$$

which is unrelated to the time-dependent nature of the state. For the ratio between the lifetimes we have $\Delta t/\tau_0=Q_0^2/|K_0|^2\ll1$. According to (7.11) the total number of pairs which have not emitted any phonons has the form $\mathcal{N}_{0n}=\hbar W_l/2\pi\Delta E$, ($|K_0|^2\gg Q_0^2$), which is $2\pi\Delta E/\hbar\gamma_0$ smaller than the number of pairs created in a real transition.

8. DISTRIBUTION FUNCTION FOR $N\geq1$ IN THE HEAVY-HOLE APPROXIMATION

Further calculations of $F_N(\mathbf{r})$ in the case $N\geq1$ become cumbersome due to the large number of symmetric diagrams. Wishing to obtain results for an arbitrarily large value of N, we consider a model in which it is assumed that $m_h\gg m_e$. If the hole effective mass m_h is very large, by increasing ω_l we can pass through the region in which the electron can actually emit several LO phonons and the hole can no longer emit any phonons. Then significant contributions to $\mathcal{F}_N(\mathbf{p})$ are made by the diagrams in which the phonon lines connect only electron lines to one another. In the limit $m_h\to\infty$ we have $\gamma_h(\mathbf{k},n)\to0$, since the reciprocal lifetime of the hole is determined not by the probability of the real emission of an LO phonon, but by other processes (for example, scattering on an impurity), which are not taken into account.

We calculate the distribution function of electron–hole pairs $F_{1nn_1}(\mathbf{r})$ after the emission of one phonon. The Fourier transform $\mathscr{F}_{1nn_1}(\mathbf{p})$ is specified by one diagram (Fig. 3b) and has the form

$$\mathscr{F}_{1nn_1}(\mathbf{p}) = |M_l|^2\left(\frac{2m_e}{\hbar^2}\right)\sum_{\mathbf{k},\mathbf{q}} |C_q|^2|M_{nn_1}|(q_z)|^2$$

$$\times\left[\left(\mathbf{k}+\frac{\mathbf{p}}{2}\right)^2-K_0^2-iQ_0^2\right]^{-1}\left[\left(\mathbf{k}-\frac{\mathbf{p}}{2}\right)^2\right.$$

$$\left.-K_0^2+iQ_0^2\right]^{-1}\left[\left(\mathbf{k}+\mathbf{q}_\perp+\frac{\mathbf{p}}{2}\right)^2\right.$$

$$\left.-K_1^2-iQ_1^2\right]^{-1}\left[\left(\mathbf{k}+\mathbf{q}_\perp-\frac{\mathbf{p}}{2}\right)^2-K_1^2+iQ_1^2\right]^{-1},$$

$$(8.1)$$

K_0 is given by Eq. (7.3), in which $\mu=m_e$, and

$$K_1\equiv K_1(n_1)=\hbar^{-1}\sqrt{2m_e(\hbar\omega_l-E_g-\hbar\omega_{\rm LO})-\hbar^2\pi^2n_1^2/d^2},$$

$$Q_1=Q_1(n_1). \qquad (8.2)$$

To obtain simpler visualizable results, we use a model in which the interaction C_q does not depend on $\mathbf{q}$ and is described by Eq. (2.9). Then the sums with respect to $\mathbf{k}$ and $\mathbf{q}$ in (8.1) separate into a product of two sums, which reduce to integrals like (7.7). The summation with respect to q_z gives

$$\sum_{q_z} |M_{nn_1}(q_z)|^2=\frac{L_z}{d}\left(1+\frac{\delta_{n,n_1}}{2}\right), \qquad (8.3)$$

where L_z is the normalization length. Taking into account (8.3) and (7.8), we represent $\mathscr{F}_{1nn_1}(\mathbf{p})$ in the form

$$\mathscr{F}_{1nn_1}(\mathbf{p})=|M_l|^2|C|^2S_0^2\frac{L_z}{d}(2\pi)^{-2}\left(\frac{2m_e}{\hbar^2}\right)^4$$

$$\times\left(1+\frac{\delta_{n,n_1}}{2}\right)\Phi_{nn_1}(p),$$

$$\Phi_{nn_1}(p)=\frac{g_n}{\sqrt{p^2+y_-^{(n)}}}\frac{g_{n_1}}{\sqrt{p^2+y_-^{(n_1)}}}. \qquad (8.4)$$

The function g_n and $y_\pm^{(n)}$ are defined in (7.8); g_{n_1} and $y_\pm^{(n_1)}$ differ from them by the replacement $K_0,Q_0\to K_1,Q_1$. According to (4.4), the distribution function $F_{1nn_1}(\mathbf{r})$ equals

$$F_{1nn_1}(\mathbf{r})=|M_l|^2|C|^2S_0^2\frac{L_z}{d}(2\pi)^{-3}\left(\frac{2m_e}{\hbar^2}\right)^4$$

$$\times\left(1+\frac{\delta_{n,n_1}}{2}\right)V_{1nn_1}(r),$$

$$V_{1nn_1}(r)=\int_0^\infty p\,dp\frac{g_ng_{n_1}J_0(pr)}{\sqrt{(p^2+y_-^{(n)})(p^2+y_-^{(n_1)})}}. \qquad (8.5)$$

The distribution function normalized to unity $f_{1nn_1}(\mathbf{r})=.\,I'_{1nn_1}F_{1nn_1}(\mathbf{r})$ has the form

$$f_{1nn_1}(\mathbf{r})=\frac{2Q_0^2Q_1^2V_{1nn_1}(r)}{\pi\arctan(-Q_0^2/K_0^2)\arctan(-Q_1^2/K_1^2)}. \qquad (8.6)$$

After the emission of one LO phonon, the probability for the electron to be at the point of creation of the electron–donor pair $\mathbf{r}=0$ decreases. This is reflected in the fact that the integral in Eq. (8.6) is nonsingular in the limit $\mathbf{r}\to 0$.

In the nonresonant case $K_j\gg Q_j$, we have $\arctan(-Q_j^2/K_j^2)=\pi$ $(j=0, 1)$, $y_-^{(n_1)}=Q_1^4/K_1^2=\lambda_1^{-2}$, $y_+^{(n_1)}=4K_1$, and, according to (8.5),

$$f_{1nn_1}(\mathbf{r})=2\pi^{-3}Q_0^2Q_1^2\int_0^\infty p\,dp\frac{g_ng_{n'}J_0(pr)}{\sqrt{(\lambda_0^{-2}+p^2)(\lambda_1^{-2}+p^2)}}. \qquad (8.7)$$

The integral in (8.7) diverges logarithmically at small A (i.e., $\lambda_j\to\infty$ for $Q_j\to 0$,; therefore, $f_{1nn_1}(0)\propto A^2\ln A^{-1}$. In the polar approximation, the replacement of g_n and g_{n_1} by their values for $p=0$ gives the expression

$$f_{1nn_1}(\mathbf{r})=\frac{1}{2\pi\lambda_0\lambda_1}\int_0^\infty p\,dp\frac{J_0(pr)}{\sqrt{(p^2+\lambda_0^{-2})(p^2+\lambda_1^{-2})}}, \qquad (8.8)$$

which is applicable when $r\gg K_j^{-1}$. We also consider the resonant case of $K_1=0$ and $K_0\gg Q_0$, i.e., the case in which the electron drops to the minimum of the band with the index n_1 after it emits a phonon (the variant with $K_0=0$ and $K_1\gg Q_1$ is obviously possible). In this case the integral in (8.6) depends on three parameters having the dimensions of length and satisfying the inequalities

$$\lambda_0\gg\Lambda_1=(\sqrt{2}Q_1)^{-1}\gg(2K_0)^{-1}.$$

If $r\gg\Lambda_1$ holds, then $f_{1nn_1}(\mathbf{r})$ is specified by (7.13) for the case of $N=0$, which, however, is valid over a broader range of values of r. In the limit $r\to 0$ we obtain $f_{1nn_1}(0)\propto A^{3/2}$, i.e., $f_{1nn_1}(0)$ is higher than in the nonresonant case, and $f_{1nn_1}(\mathbf{r})$ decreases with r more rapidly than does the nonresonant function. The condition $\omega_{\rm LO}=(\hbar\pi^2/m_ed^2)\times(n_1^2-n^2)$ can be satisfied by adjusting the parameters of the quantum well. Double resonance is then realized: $K_0=K_1=0$. It can be shown from the general formula (8.6) that $f_{1nn_1}(0)\propto A$, i.e., a further increase in $f_{1nn_1}(0)$ occurs. Plots of $f_{1nn_1}(\mathbf{r})$ calculated from Eqs. (8.5) and (8.6) are presented in the inset in Fig. 4. An increase in $f_{1nn_1}(0)$ is seen upon passage from the nonresonant case (curve d) to the resonant case (curves c and b) and to double resonance (curve a). Figure 5 shows the electron transitions corresponding to curves a–d.

In the case of $N\geq 2$ the functions $\mathscr{F}_{Nnm}(\mathbf{p})$ correspond to diagrams of two types, examples of which are presented in Fig. 6. In one of them the phonon lines do not intersect one another, and in the other they do intersect. It can be shown that diagram 6b contains an extra coupling constant in the numerator in comparison with diagram 6a. Thus, it is sufficient to take into account only the noninterference contributions, i.e., for a given N the functions $\mathscr{F}_{Nnn_1}$ correspond to a single diagram. As is seen from Fig. 6a, $\mathscr{F}_{2nn_1}$ is a double sum with respect to the quantum numbers ν and ν'. How-
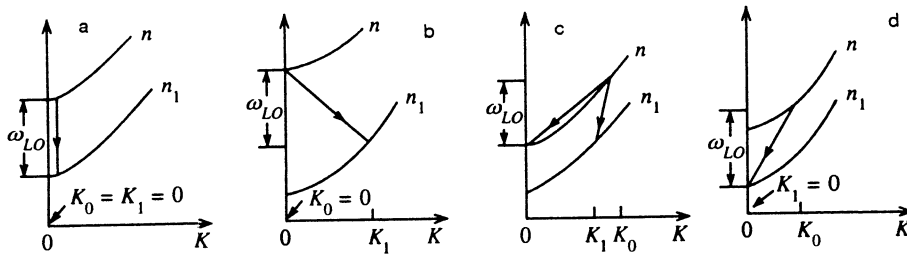
FIG. 5. Transitions between size-quantization bands n and n_1 corresponding to curves a–d in the inset in Fig. 4. The frequency is plotted along the vertical axis on an arbitrary scale.

ever, the off-diagonal terms in the sum have smaller coupling constants than do the diagonal terms. Their small values are attributed to the fact that in the case of $\nu \neq \nu'$ the expression for $\mathscr{F}_{2nn_1}$ contains the multipliers

$$[(\mathbf{k}+\mathbf{q}_\perp+\mathbf{p}/2)^2 - K_j^2(\nu) - iQ_\nu^2]^{-1}$$

$$\times[(\mathbf{k}+\mathbf{q}_\perp-\mathbf{p}/2)^2 - K_j^2(\nu') - iQ_{\nu'}^2]^{-1},$$

where $K_j(\nu) \neq K_j(\nu')$, which leads to a smaller contribution in comparison with the case of $\nu = \nu'$. For this reason the diagram in Fig. 6b makes a smaller contribution than that in Fig. 6a. Thus, in any diagram the indices of the electron lines on the right- and left-hand sides are in pairwise agreement. After the simplifications described above, the distribution function normalized to unity is given by the expression

$$f_{N\beta}(\mathbf{r}) = \frac{2^N \mathscr{D}_\beta}{\pi} \int_0^\infty \frac{p\, dp\, J_0(pr) g_{n_0} \cdots g_{n_N}}{\sqrt{(p^2 + y_-^{(n_0)}) \cdots (p^2 + y_-^{(n_N)})}},$$

$$\mathscr{D}_\beta = Q_{n_0}^2 \cdots Q_{n_N}^2 [\arctan(-Q_{n_0}/K_0^2) \cdots \arctan(-Q_{n_N}/K_N^2)]^{-1},$$

$$K_i \equiv K_i(n_i) = \hbar^{-1}\sqrt{2m_e(\hbar\omega_l - E_g - i\hbar\omega_{LO}) - \hbar^2\pi^2 n_i^2/d^2},$$

$$y_\pm^{(n_i)} = 2(\sqrt{K_i^4 + Q_{n_i}^4} \pm K_i^2). \tag{8.9}$$

The index $\beta = n_0, \cdots, n_N$ corresponds to the size-quantization bands into which the electron passes as it emits N phonons, and the index i denotes the number of phonons emitted after the transition to band n_i.

In the nonresonant case, beginning at $N=2$, the use of the polar approximation leads to the expression

$$f_{N\beta}(\mathbf{r}) = \frac{1}{2\pi\lambda_{n_0}\cdots\lambda_{n_N}} \int_0^\infty \frac{p\, dp\, J_0(pr)}{\sqrt{(p^2 + \lambda_{n_0}^{-2}) \cdots (p^2 + \lambda_{n_N}^{-2})}},$$

$$\lambda_{n_i} = \frac{K_i}{Q_{n_i}^2},$$

whence it follows that $f_{N\beta}(0) \propto A^2$. At resonance, where one of the K_i (for example, K_N) vanishes, we replace all the g_{n_i} in the general equation (8.9) except $g_{n_N}(p^2)$ by $g_{n_i}(0)$. After this replacement and the transition to the integration variable $x = p/Q_{n_N}$, we obtain

$$f_{N\beta}(\mathbf{r}) = \frac{2C_0}{\pi^2} \int_0^\infty \frac{x\, dx\, J_0(Q_{n_N} r x)}{\sqrt{(x^2 + \zeta_0^2)\cdots(x^2 + \zeta_{N-1}^2)}} \frac{g_{n_N}'(p^2)}{\sqrt{|x^4 - 4|}},$$

$$\zeta_i = \lambda_{n_i}^{-1} Q_{n_N}^{-1}, \tag{8.10}$$

$$C_0 = (Q_{n_N}^{N-2}\lambda_{n_0}\cdots\lambda_{n_{N-1}})^{-1} \propto A^{1+N/2}.$$

For $\zeta_i \propto \sqrt{A} \to 0$ the integral in (8.10) diverges at the lower limit as $A^{1-N/2}$, if we have $N \geq 3$, i.e., $f_{N\beta}(0) \propto A^2$, as in the nonresonant case. For $N=2$ we have $f_{N\beta}(0) \propto A^2 \ln A^{-1}$.

9. DISCUSSION OF RESULTS

The general theory presented above makes it possible to calculate both the wave function of an electron–hole pair which has emitted N LO phonons and distribution functions of other types. Apart from the distribution functions of the relative distance between an electron and a hole in the plane of a quantum well and the total number of electron–hole pairs which have emitted N LO phonons, which were considered in the present work, $F_{Nnmn'm'}(\mathbf{r}, \mathbf{K})$, which is related to the scattering tensor, can be calculated.

The distribution function for $N=0$ was calculated exactly and describes the distribution of electron–hole pairs for arbitrary electron and hole effective masses in the range of frequencies of the exciting light corresponding to both the real and virtual creation of a pair. The distribution functions for $N \geq 1$ were calculated with a model interaction and in the heavy-hole approximation. These simplifications made it possible to calculate the distribution functions over a broad range of values of K_i down to $K_i = 0$, which corresponds to the resonant case, in which the electron drops to the minimum of the size-quantization band in one of the transitions. The resonant distribution function decreases with the distance more rapidly than the nonresonant analog, but this difference is compensated by the fact that at small $\mathbf{r}$ it is larger than the nonresonant function. The distribution functions depend on the wandering trajectory of the electron among the size-quantization bands during phonon emission.

According to (8.3), in the model interaction each transition with phonon emission has a multiplier equal to 3/2, if the transition occurs within a single band, and a multiplier
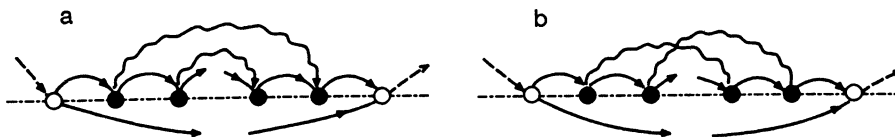

FIG. 6. Examples of diagrams for $\mathscr{F}_{2n_0n_1n_2}(\mathbf{p})$ without interaction (a) and with intersection (b) of the phonon lines.

equal to unity, if the bands are different. If the bands change in each electron transition, the smallness of $(2/3)^N$ becomes a factor. In the case of a Fröhlich interaction, the constant (8.3) after the integration with respect to the variables q_{iz} is replaced by functions of $q_{i\perp}$, which are smaller than the constant (8.3) over the entire range of values of $q_{i\perp}$. This should make the off-diagonal contributions small. They are smaller, the larger is the difference between the quantum numbers in the electron transition. Thus, the main contribution to

$$F_N(\mathbf{r}) = \sum_\beta F_{N\beta}(\mathbf{r})$$

is made by the parts of the sum which are diagonal with respect to all the band indices. These assessments also apply to $F_N(\mathbf{r},\mathbf{K})$, which is related to the scattering tensor. The numerical smallness of the off-diagonal contributions is attributed to the interference of the wave functions (2.2).

The heavy-hole approximation drastically reduces the number of diagrams which must be taken into account in calculating the distribution functions. The distribution functions for $N \geq 1$ obtained above take into account only the real processes of LO-phonon emission and pair creation. Consideration of the virtual processes would expand the range of values of ω_l in which the distribution function is defined. This would require consideration of the virtual emission of LO phonons by a heavy hole.

The model of a quantum well underlying the theory developed above is idealized, since it does not take into account the imperfect nature of the boundaries of the well and the finite nature of its depth. Also, exciton states are not taken into account as intermediate states, in which the electron and hole might be found during the emission of phonons. The deviation of the form of the well boundaries from planarity complicates the problem of determining the spectrum of the electron and the hole. However, modern methods for growing heterostructures are sufficiently perfected and practically rule out the appearance of roughness; therefore, the boundaries may be considered planar with good accuracy. The characteristic depth of a well U equals 0.4–0.6 eV. In order for the model of a well with infinitely high potential walls to correspond to reality, the following inequalities must be satisfied:

$$\hbar \gamma_e < \hbar^2 \pi^2 / 2 m_e d^2 \ll U.$$

If it is assumed that $d = 2 \times 10^{-6}$ cm, $m_e = 0.1 m_0$, $\alpha = 3 \times 10^{-2}$, and $\omega_{LO} = 2 \times 10^{13}$ s^{-1}, we have $\hbar \gamma_e$

$$\approx 2 \alpha l \omega_{LO}^2 m_e d / \pi = 4.6 \times 10^{-4} \quad \text{eV, and} \quad \hbar^2 \pi^2 / 2 m_e d^2$$
$$= 9.7 \times 10^{-3} \text{ eV. Thus, in a quantum well with a depth of}$$
0.5 eV there are six to seven size-quantization levels, and they are not smeared by the interaction with LO phonons.

The intermediate exciton states must be taken into account near the points of exciton resonance $\hbar \omega = E_{ex}$, where E_{ex} is the exciton energy measured from the ground-state energy of the crystal. The inclusion of exciton states in the theory of multiphonon resonant Raman scattering is a problem in its own right and requires a separate analysis. Here we only note that diagrams in which the last and next-to-last intermediate states are exciton states make an appreciable contribution to the distribution function and the scattering tensor.

[1] M. Cardona, in Light Scattering in Solids, edited by M. Cardona and G. Güntherodt, Springer, Heidelberg, 1982, Vol. 2, p. 19.

[2] R. Merlin, G. Güntherodt, and R. Humphery, in Physics of Semiconductors: Conference Series Number 43, edited by B. L. Wilson, IOP Conference Proceedings, Institute of Physics and Physical Society, London, 1979, p. 683.

[3] M. Yoshida, N. Ohno, H. Mitsutake et al., J. Phys. Soc. Jpn. 54, 2754 (1985); N. Ohno, M. Yoshida, K. Nakamura, and Y. Nakai, Solid State Commun. 53, 569 (1985).

[4] V. T. Hou, Y. Jin, M. Y. Shen et al., Superlattices Microstruct. 12, 69 (1992).

[5] R. Zeyher, Solid State Commun. 16, 49 (1975).

[6] A. V. Goltsev, I. G. Lang, S. T. Pavlov et al., J. Phys. C 16, 4221 (1983).

[7] V. I. Belitskiĭ, A. V. Gol'tsev, I. G. Lang, et al., Zh. Éksp. Teor. Fiz. 86, 272 (1984) [Sov. Phys. JETP 59, 155 (1984)].

[8] L. I. Korovin, S. T. Pavlov, and B. É. Éshpulatov, Zh. Éksp. Teor. Fiz. 99, 1619 (1991) [Sov. Phys. JETP 72, 904 (1991)]; Pis'ma Zh. Éksp. Teor. Fiz. 51, 516 (1990) [JETP Lett. 51, 584 (1990)].

[9] L. I. Korovin, S. T. Pavlov, and B. É. Éshpulatov, Fiz. Tverd. Tela (St. Petersburg) 35, 1562 (1993) [Phys. Solid State 35, 788 (1993)].

[10] V. I. Belitsky, I. G. Lang, and S. T. Pavlov, Physica B 172, 452 (1991).

[11] I. G. Lang, S. T. Pavlov, and O. Sotolongo Costa, Fiz. Tverd. Tela (St. Petersburg) 34, 579 (1992) [Sov. Phys. Solid State 34, 310 (1992)].

[12] L. I. Korovin, S. T. Pavlov, and B. É. Éshpulatov, Fiz. Tverd. Tela (St. Petersburg) 34, 1293 (1992) [Sov. Phys. Solid State 34, 683 (1992)].

[13] V. I. Belitsky, M. Cardona, I. G. Lang et al., Phys. Rev. B 46, 15 767 (1992).

[14] E. L. Ivchenko, I. G. Lang, and S. T. Pavlov, Fiz. Tverd. Tela (Leningrad) 19, 1227 (1977) [Sov. Phys. Solid State 19, 718 (1977)].

[15] E. L. Ivchenko, I. G. Lang, and S. T. Pavlov, Phys. Status Solidi B 85, 81 (1978).

[16] I. G. Lang, S. T. Pavlov, A. V. Prokaznikov et al., Phys. Status Solidi B 127, 187 (1985).

Translated by P. Shelnitz